

Time-Base Nonlinearity Determination Using Iterated Sine-Fit Analysis

Gerard N. Stenbakken and John P. Deyst

Electricity Division, U. S. National Institute of Standards and Technology¹,
Gaithersburg, MD 20899, USA

Phone (301) 975-2440, Fax (301) 926-3972, email stenbakken@eeel.nist.gov

Abstract – A new method is presented to determine the time-base errors of sampling instruments. The method does not require a time-base error model and thus provides accurate estimates where model-based methods fail. Measurements of sinewaves at multiple phases and frequencies are used as test signals. A harmonic distortion model is used to account for amplitude nonlinearity of the sampling channel. Use of an independent method for estimating the channel noise and jitter allows an accurate estimate of the harmonic order. Methods are presented for separating the harmonics generated by the sampling channel from those generated by the time-base distortion. The use of an iterative sine-fit procedure gives accurate results in a short time. A new weighting procedure is described, which minimizes the error in the estimates. Guidelines are given for selecting good sets of test frequencies. Results are shown for both simulated and real data.

I. INTRODUCTION

Deviations in the sample intervals of sampling instruments cause nonlinear distortion of the sampled waveforms. If these deviations can be measured, corrections can be made to the sampled data, or the sampling intervals can be modified to correct them. The sample interval deviations have two components; a deterministic part called time-base distortion, and a random component called jitter.

A number of methods have been developed to measure time-base distortion. The "zero-crossing" methods [1-3] make use of waveforms of constant frequency, or carefully selected frequencies [4]. The resolution of these techniques is equal to the sine period, so they are limited by the bandwidth of the sampling channel. Early "sinefit" methods assumed a pure sinewave input signal [5]; these methods do not easily handle harmonic distortion caused by the sampling channel of the instrument. An improved sinefit method [6] is able to account for the harmonic distortion of the sampling channel. A time-base distortion determination method using the improved

sinefit method has been developed [7]. A phase demodulation technique called the "analytic signal" method [8] has also been described. Both the improved sinefit and analytic signal methods use models for the time-base distortion, which prevent them from accurately estimating discontinuities in the time-base distortion, as shown in [9].

This paper describes a new method for determining time-base distortion, based on iterating the sine-fitting process. Because a time-base error model is not used, this method can accurately estimate discontinuities in the time-base. A harmonic model is used to account for the amplitude nonlinearity of the sampling channel, which allows determination of the distortion of the input signal or distortion caused by the channel. Use of the proper harmonic order is important for accurate time-base distortion estimation. If the model order is too low, some channel distortion will be attributed to the time-base error, and, if the model order is too high, some noise will be fit as channel distortion also increasing the time-base error. A method for determining the proper harmonic order is described that compares the sine-fit residuals to an independent assessment of the noise and jitter of the measurement process.

Time-base distortion estimates depend on the time derivative of the input signal. Where this derivative is small, the additive noise can either make the process unstable or make the estimates inaccurate. To overcome this problem, various weighting methods have been tried. Three are described here and one, a new weighting method, is shown by simulation to give the most accurate time-base distortion estimates. Since both nonlinear channel electronics and time-base distortions can generate harmonic distortions, the time-base estimation method must be able to distinguish the causes. Two methods are described for resolving this ambiguity; use of either two or more frequencies or a constant-waveshape constraint. Guidelines are given for good frequency pairs to use for good harmonic ambiguity resolution.

¹ Technology Administration, U. S. Department of Commerce

where the $2h + 1$ parameters are the least squares solution from fitting (6) to $s_m^j(k)$. Eqn.(7) is iteration $i = 0$. Successive iterations are given by fitting

$$s_{ei}^j(t_{ki}) = A_{0i}^j + \sum_{l=1}^h A_{li}^j \sin(l\omega^j t_{ki} + \phi_{li}^j) \quad (8)$$

to $s_m^j(k)$, where

$$t_{k(i+1)} = t_{ki} + \frac{T_s}{w_T(k)} \sum_{j=1}^M w^j(k) g_i^j(k), \quad (9)$$

$$w_T(k) = \sum_{j=1}^M w^j(k), \quad (10)$$

and

$$g_i^j(k) = \frac{s_m^j(k) - s_{ei}^j(t)}{T_s \dot{s}_{ei}^j(t)} \Big|_{t=t_{ki}}. \quad (11)$$

The weighting factors $w^j(k)$ are discussed in Section III. At each iteration the fit error K_ϵ is calculated as

$$K_{\epsilon i} = \left(\frac{1}{D_F} \sum_{j=1}^M \sum_{k=0}^{N-1} (s_m^j(k) - s_{ei}^j(t_{ki}))^2 \right)^{\frac{1}{2}}, \quad (12)$$

where $D_F = MN - N - 2h - 1$, is the degrees of freedom. The iterations are stopped when the change in the fit error is below some tolerance δ_I , i.e., when $K_{\epsilon(i-1)} - K_{\epsilon i} \leq \delta_I$, or when the number of iterations has reached a limit n_I . The value of the fit error at convergence is called K_F , the final values for the sample time estimates from (9) are called \hat{t}_k , and the time-base distortion estimates are given by $\hat{g}(k) = (\hat{t}_k - kT_s) / T_s$.

D. Constant-Waveshape Constraint Method

Constant-waveshape constraint, the second method for removing the harmonic ambiguity, assumes that for different phases the waveform harmonic amplitudes and relative phases remain constant. This method of removing the harmonic ambiguity can be used together with the multiple frequency method. Thus, the description below assumes that the records are ordered into constant frequency groups and that this constraint is applied to the sampled waveforms in each frequency group. Since harmonic distortion is normally amplitude and frequency dependent, we assume that the p_f waveforms in each group have constant amplitude and frequency. Exactly how closely the amplitudes and frequencies must be maintained is dependent on how sensitive the harmonics are to these parameters. This will not be discussed here other than to point out that the signal frequencies are not a fitted parameter in this analysis and the error in the relative signal frequencies is assumed small compared to the jitter standard deviation relative to the record length.

The estimated harmonic amplitudes and phases for each group are averaged and the average amplitude and phase are

used in the estimate for the time-base distortion. This is done by first decomposing each harmonic into a sinewave that crosses zero in phase with the fundamental plus a sinewave in quadrature. Thus, the fit estimates are given as

$$s_{e0}^j(t_{k0}) = A_{00}^j + A_{10}^j \sin(\omega^j t_{k0} + \phi_{10}^j) + \sum_{l=2}^h B_{l0}^j \sin(l\omega^j t_{k0} + l\phi_{10}^j) + C_{l0}^j \cos(l\omega^j t_{k0} + l\phi_{10}^j), \quad (13)$$

where

$$B_{l0}^j = A_{l0}^j \cos(\phi_{l0}^j - l\phi_{10}^j), \quad (14)$$

and

$$C_{l0}^j = A_{l0}^j \sin(\phi_{l0}^j - l\phi_{10}^j). \quad (15)$$

The B_{l0}^j and C_{l0}^j for each group are averaged. The constrained constant-waveshape fits \bar{s}_{e0}^j are obtained by using these average values \bar{B}_{l0}^j and \bar{C}_{l0}^j in place of the individual harmonic amplitudes in (13) for all waveform estimates in each group. The constrained time-base distortion estimates at each iteration are given by

$$\bar{g}_i^j(k) = \frac{s_m^j(k) - \bar{s}_{ei}^j(t)}{T_s \dot{\bar{s}}_{ei}^j(t)} \Big|_{t=t_{ki}}. \quad (16)$$

Note that in this implementation, the amplitudes of the fundamental in each group are not averaged. These values should be checked after convergence to verify that they are constant for all waveforms within each group.

III. SIMULATION RESULTS

To apply these methods, some of the questions that need to be addressed are what harmonic order h and frequencies ω^j to use in (8) or (13), and what weighting factors $w^j(k)$ to use in (9). The appropriate harmonic order can be determined by looking at K_F as a function of h , $K_F(h)$. As h is increased $K_F(h)$ will decrease then level off at the proper h value. The expected value at which $K_F(h)$ should level off can be estimated from the standard deviation of repeat measurements of $s_m(k)$. Take M_R records of one phase of the input signal $s_m^j(k)$, $j = 1$ to M_R ; then calculate the RMS of the standard deviations at each sample $\bar{\sigma}_{M_R}$ as

$$\bar{\sigma}_{M_R} = \left(\frac{1}{N} \sum_{k=0}^{N-1} \hat{\sigma}_{M_R}^2(k) \right)^{\frac{1}{2}}, \quad (17)$$

where

$$\hat{\sigma}_{M_R}^2(k) = \frac{1}{M_R - 1} \sum_{j=1}^{M_R} (s_m^j(k) - \bar{s}_m(k))^2, \quad (18)$$

and

$$\bar{s}_m(k) = \frac{1}{M_R} \sum_{j=1}^{M_R} s_m^j(k). \quad (19)$$

The value at which $K_F(h)$ levels off should be close to $\bar{\sigma}_{M_R}$. As shown in [6] the estimated sample standard deviations

errors was made from 100 repeat records of a signal with 23 Hz, 0 degrees phase. Following [6], analysis of these records gives a repeat RMS standard deviation $\bar{\sigma}_{MR}$ of 10.1 mV and noise and jitter standard deviations $\hat{\sigma}_d = 10$ mV and $\hat{\sigma}_\tau = 16$ μ s. All three values are close to the expected values. The value at which K_F leveled off, 9.8 mV, is approximately the repeat RMS standard deviation, 10.1 mV.

TABLE II.
COMPARISON OF THE TIME-BASE ESTIMATE AND FIT ERRORS
FOR DIFFERENT HARMONIC MODELS

Harmonics	K_F	T_{RMS}
{1}	70.5 mV	450 μ s
{1,2}	12.0 mV	64 μ s
{1,2,3}	9.8 mV	52 μ s
{1,2,3,4}	9.7 mV	53 μ s

C. Frequency Selection

The choice of appropriate input signal frequencies to give good discrimination between harmonics caused by the sampling channel and time-base distortion can be decided by looking at pairs of frequencies. For the three-harmonic signal model used in the above simulation, the RMS error in the time-base estimates T_{RMS} was simulated for many frequency pairs. The fit model used was the correct three-harmonic model. As above, four records were used with two phases, 0 and 90 degrees, for each of the two frequencies. Fig. 2 shows by an intensity plot of $\log_{10}(T_{RMS})$, with a very small amount of noise and jitter added. This plot shows the matrix of frequency pairs obtained by varying each frequency from 1 Hz to the Nyquist frequency, $f_N = 32$ Hz. The intensities of

the pixels are darker for frequency pairs that are good (lower T_{RMS}) and lighter for pairs not so good. The lighter diagonal lines delineate frequency pairs not to use. As the order of the fit model increases, more such lines appear on this kind of plot. The main diagonal shows the obvious poor choice of using pairs with the same frequency. Another line starting from the upper left below the main diagonal shows that one frequency f_1 should not be half the other frequency f_2 when the fit model contains second harmonics. Lines from the upper right shows that f_1 should not be the alias of f_2 , $f_N - f_2$, nor twice the alias of f_2 . A second but less bright set of lines show that the frequencies and aliases should not be related by a factor of 3 or a factor of 3 plus the sampling frequency f_s .

Fig. 3 is a similar plot with the constant-waveshape constraint applied. Even though there are only two phases in each group, this constraint has significantly reduced the error in the time-base estimates. While the diagonal lines have been reduced in intensity, several horizontal and vertical lines have appeared. These show that when the constant-waveshape constraint is applied, neither frequency should be one-third, one-fifth or two-fifths the sampling frequency.

Some quality control parameters that are provided by this method will be briefly mentioned. For both these simulations the fit errors track the RMS time-base errors and thus can be used as a quality check on the proper selection of frequencies and phases. Also the lack of convergence within the iteration limit n_b , as happened for most of the pairs shown in light intensity on Figs. 2 and 3, indicate a poor data set.

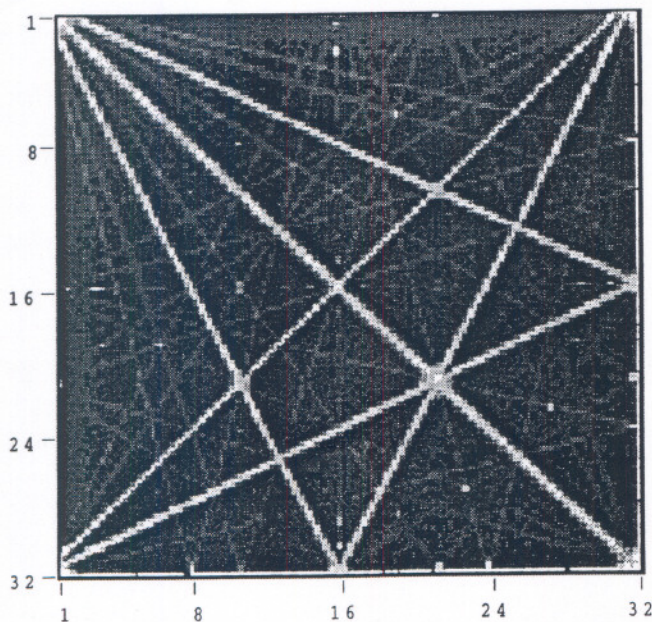


Fig. 2. Intensity plot of \log_{10} of the RMS time-base estimate errors, without constraint, axes show two frequencies in Hz.

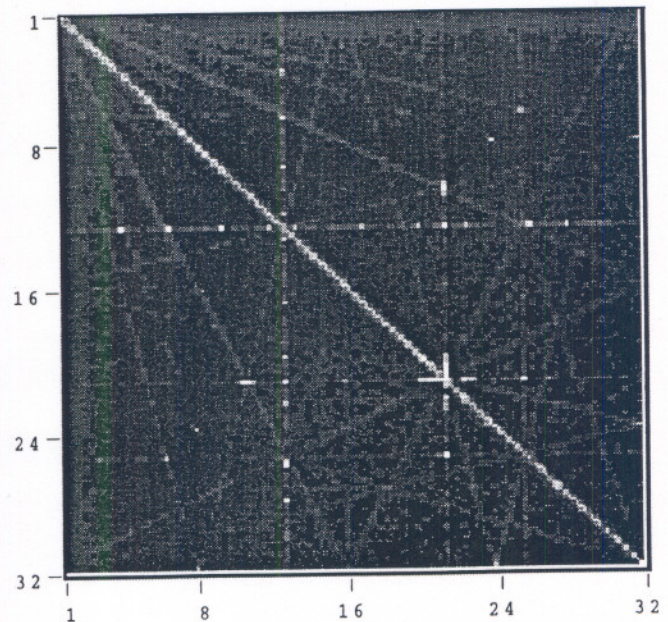


Fig. 3. Intensity plot of \log_{10} of the RMS time-base estimate errors, with constant-waveshape constraint, axes show two frequencies in Hz.